PNAS

Supplementary Information for
SARS-CoV-2 accessory proteins ORF7a and ORF3a use distinct mechanisms to downregulate MHC-I surface expression

Najla Arshad[1], Maudry Laurent-Rolle[1,2], Wesam S Ahmed[4], Jack Chun-Chieh Hsu[1], Joanna Pawlak[1,2], Debrup Sengupta[1], Susan M Mitchell[1], Kabir H Biswas[4], Peter Cresswell[1,3*]

* Peter Cresswell
Email: peter.cresswell@yale.edu

This PDF file includes:

Figures S1 to S10
Tables S1 to S2

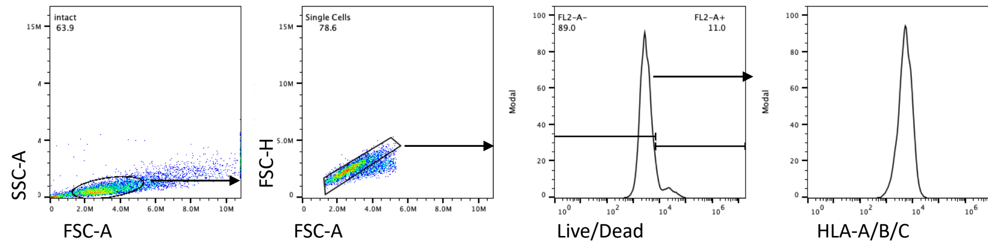

Fig. S1: Representative gating strategy for FACS analysis of MHC-I (HLA-A/B/C) in SARS-CoV-2_{WA1} -infected Vero E6 or HEK293T-hACE2 cells.

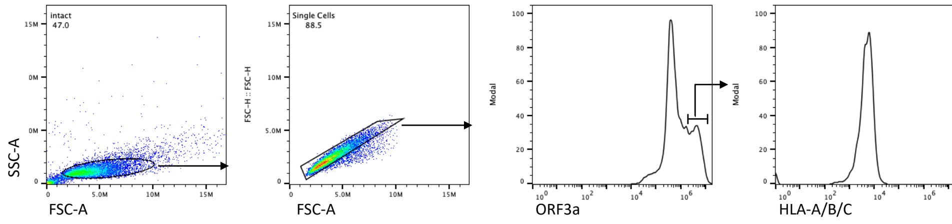

Fig. S2: Representative gating strategy for FACS analysis of MHC-I (HLA-A/B/C) in cells transfected with accessory proteins, with ORF3a as an example.

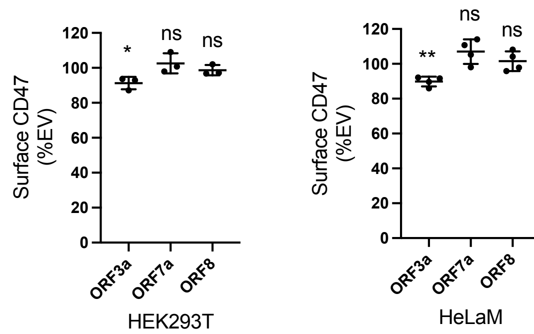

Fig. S3: Expression of surface glycoprotein CD47 is downregulated by ORF3a. Transient expression of ORF3a, ORF7a and ORF8 in HEK293T (n = 3) or HeLaM (n = 4) cells was carried out followed by flow cytometric analysis of CD47 expression 24 h post transfection. Quantitative data shown are mean $\pm$ S.D. (error bars). Statistical significance was evaluated using the unpaired Student's t test; *$p < 0.05$; **$p < 0.01$; ***$p < 0.001$; ****$p < 0.0001$; ns, not significant.

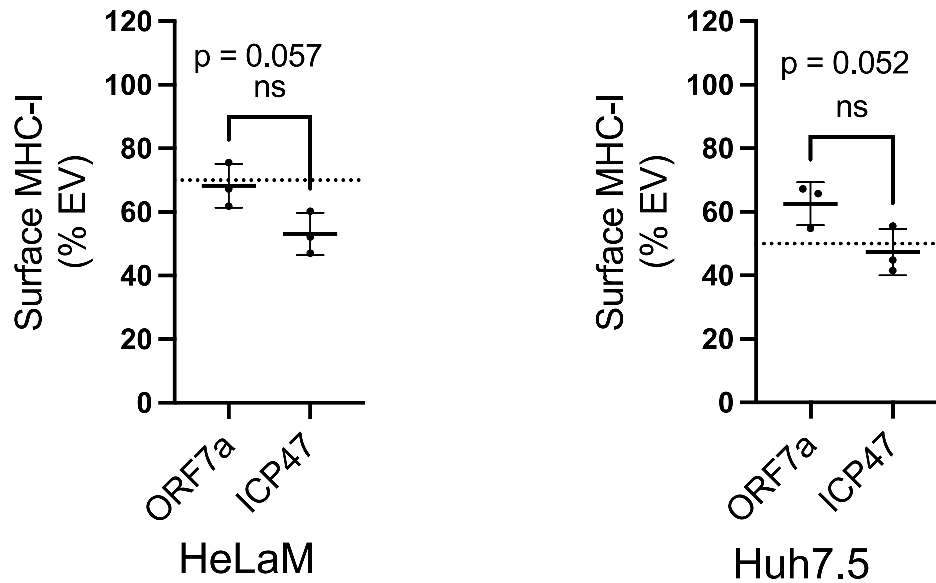

Fig. S4: Expression of surface MHC-I is downregulated by ICP47 and ORF7a. Transient expression of ICP47 or ORF7a HeLaM (n = 3) or Huh7.5 (n = 3) cells was carried out followed by flow cytometric analysis of MHC-I surface expression in transfected cells after 24 h. Quantitative data shown are mean ± S.D. (error bars). The dashed line indicates the 70% mark for HeLaM and 50% for Huh7.5. Statistical significance was evaluated using the unpaired Student's t test; *p < 0.05; **p < 0.01; ***p < 0.001; ****p < 0.0001; ns, not significant.

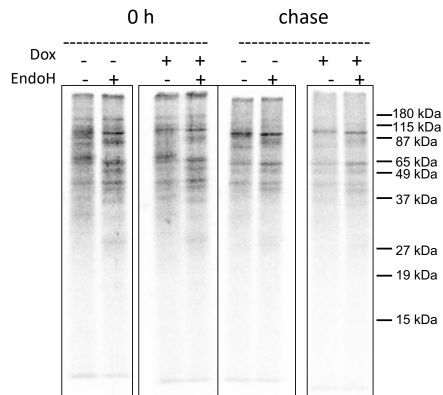

Fig. S5: Overall glycoprotein export is not affected by the expression of ORF7a. Uninduced (-Dox) or induced (+Dox for 24 h) cells were labeled with [^{35}S]Met for 15 min followed by the pull down of glycoproteins using the lectin Concanavalin A (ConA) conjugated to beads from the lysates at 0 h and 4 h of chase, followed by treatment with endoglycosidase H (EndoH). Samples were visualized after separation on nonreducing SDS-polyacrylamide gels by autoradiography.

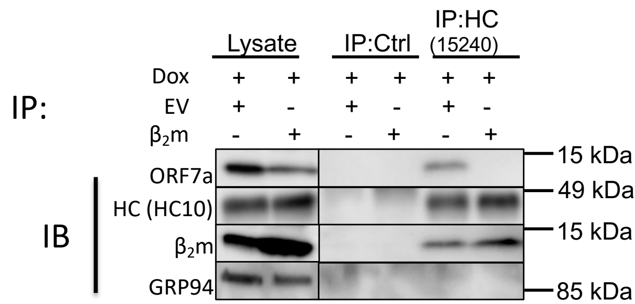

Fig. S6: Interaction between ORF7a and MHC-I was assessed by co-immunoprecipitation analysis. Total heavy chain (free and complexed) was immunoprecipitated from induced HeLaM-iORF7a cells where human β_2m was transiently transfected for 24 hours. Cells lysates were prepared in 1% digitonin and immunoprecipitation using normal IgG as a control (IP:Ctrl) or α-HLA-A/B/C, clone 15240 (IP: HC: 15240) was carried out, followed by western blot analysis to detect ORF7a, MHC-I heavy chain (HC), β_2m, or GRP94 as loading control.

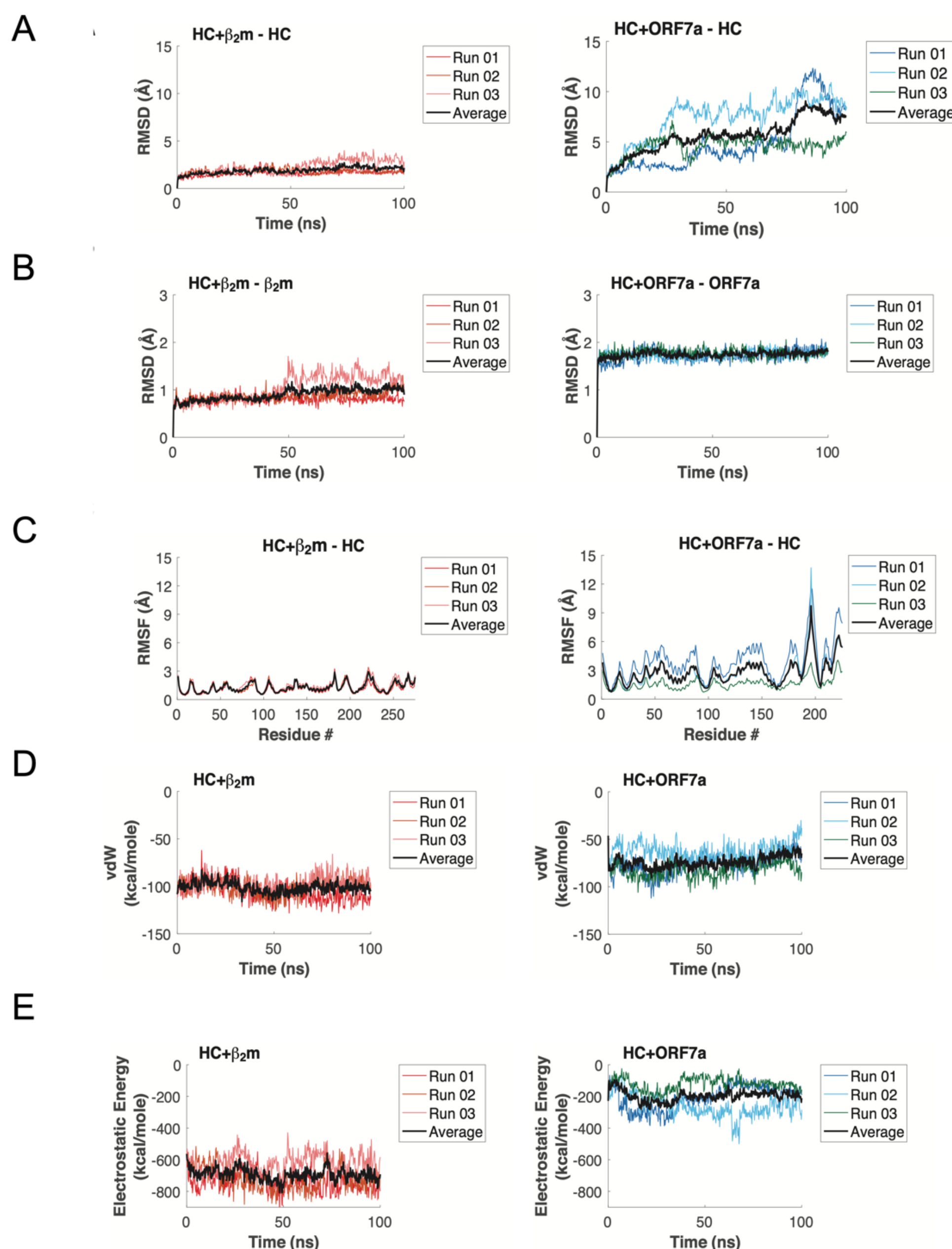

Fig. S7: Analysis of MD simulation trajectories. (A,B) Graphs showing root mean squared deviation (RMSD) of Cα atoms of the heavy chain (HC) (A) and either β2m (left panel) or ORF7a (right panel) (B) in the HC+β2m and HC+ORF7a complexes over three independent 100 ns simulations. (C) Graphs showing root mean squared fluctuation (RMSF) of Cα atoms of HC when associated with either β2m (left panel) or ORF7a (right panel) over three independent 100 ns simulations. (D,E) Graphs showing van der Waal (D) and electrostatic (E) energies of the HC+β2m (left panel) and HC+ORF7a (right panel) over the course three independent 100 ns simulations. Black lines in each graph show the average values of the indicated parameter calculated from all three MD simulation runs.

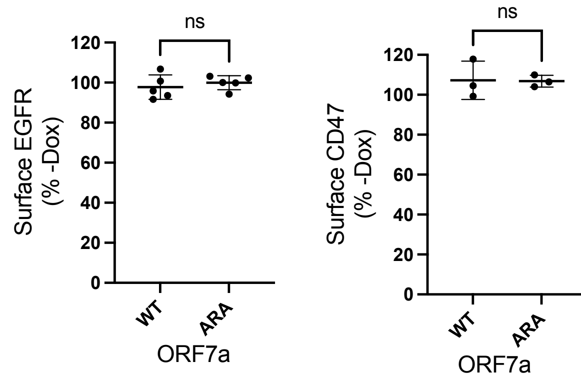

Fig. S8: Flow cytometric analysis of surface EGFR (left) and CD47 (right) levels in induced HEK293T-hAce2 cells+ORF7a-WT and HEK293T-hAce2 cells+ORF-7a-ARA cells (+Dox for 24 h), plotted relative to uninduced cells (-Dox).

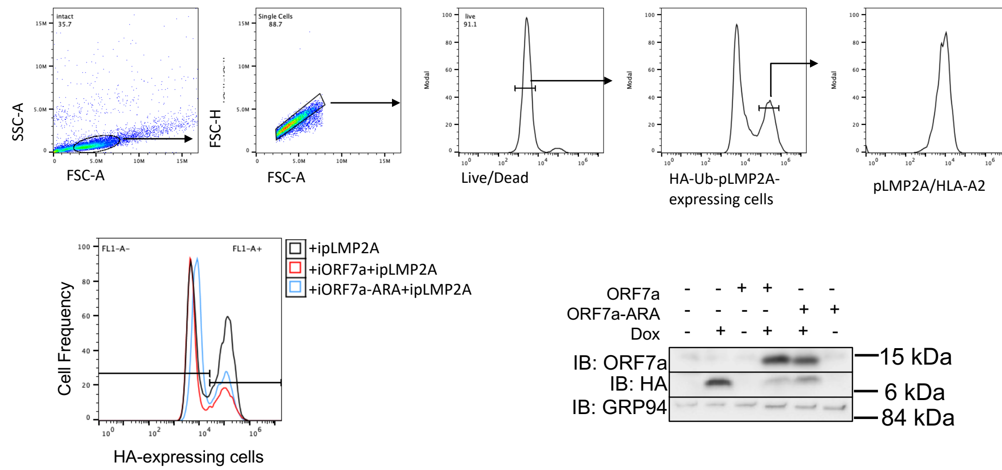

Fig. S9: Representative gating strategy for the FACS analysis of p-LMP2A-HLA-A2 complexes in the various cell lines (top). Proportion of cells expressing HA-Ub-pLMP2A fusion protein in induced cells and accompanying western blot analysis showing expression of ORF7a, HA-Ub-pLMP2A and GRP94 as loading control, in uninduced and induced cells (+Dox for 24 h, below).

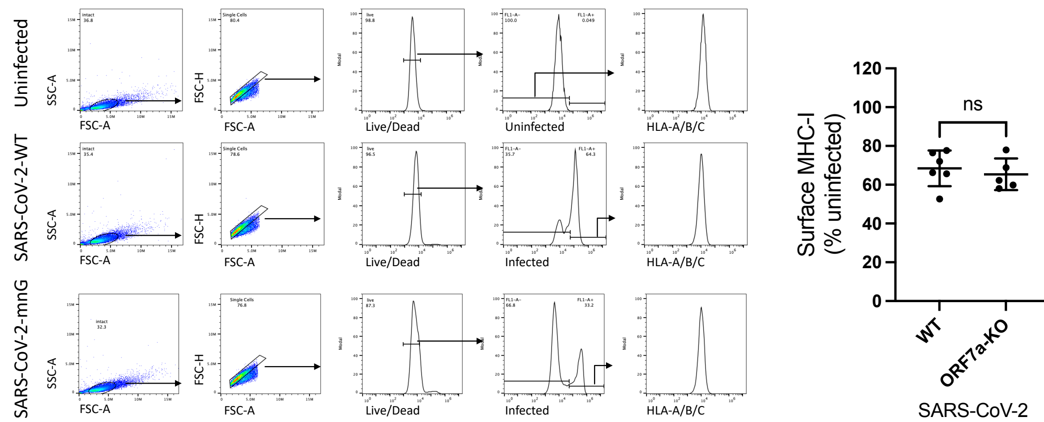

Fig S10: Infection with SARS-CoV-2 virus expressing or not expressing ORF7a does not alter MHC-I downregulation. Vero E6 or HEK293T-Ace2 cells were infected with SARS-CoV-2$_{WA1}$ or recombinant SARS-CoV-2 expressing fluorescent protein mNeoGreen (CoV-2-mNG, effectively an knockout of ORF7a) (42) (MOI = 10). 24 h post infection, cells were collected for flow cytometry analysis for surface MHC-I (n = 4). Cells infected the WT virus were identified by intracellular staining for spike protein and fluorescence from NeonGreen was used to identify cells infected with the ORF7a-null virus. Mean fluorescence intensity of MHC-I staining with W6/32 was normalized to uninfected group.

Table S1. Primers used in the generation of various plasmids used in the study

Clone name	Primer name	Sequence (5' -3')
pCAGGS-ORF3a	ORF3a-f	GGCAAAGAATTCACCATGGATTTGTTTATGAGAATCTTCACAATTGGAACTGTAACTTTGAAGCAAGG
	NoTag-r	CATGGTGAATTCTTTGCCAAAATGATGAGACAGCACAATAACC
pCAGGS-ORF7a	ORF7a-f	GGCAAAGAATTCACCATGAAAATTATTCTTTTCTTGGCACTGATAACACTCGCTACTTG
	NoTag-r	CATGGTGAATTCTTTGCCAAAATGATGAGACAGCACAATAACC
pCAGGS-ORF7a-ARA	ARA-f	CACACTCGCAAGAGCGACAGAATGAGCTAGCAGATCTTTTTCCC
	ARF-R	TCATTCTGTCGCTCTTGCGAGTGTGAAGCAAAGTGTTATAAACACTATTGC
pCAGGS-ORF8	ORF8-f	GGCAAAGAATTCACCATGAAATTTCTTGTTTTCTTAGGAATCATCACAACTGTAGCTGC
	ORF8-r	CATGGTGAATTCTTTGCCAAAATGATGAGACAGCACAATAACC
pTRIPZ-puro-ORF7a	IndORF7a-f	TAGTGAACCGTCAGATCGCACCGGTATGAAAATTATTCTTTTCTTGGC
	IndORF7a-r	GCCACGCCTCGAGACGCGTGTCATTCTGTCTTTCTTTTGAGTG
pTRIPZ-puro-ORF7a-ARA	IndORF7a-ARA-r	GCCACGCCTCGAGACGCGTGAATTCTCATTCTGTGGCTCTGGC
pTRIPZ-puro-HA-Ub	HAUb-f	TAGTGAACCGTCAGATCGCACCGGTATGTACCCATACGATGTTCCG
	HAUb-r	GCCACGCCTCGAGACGCGTGAATTCACCACCTCTCAGACG
pTRIPZ-puro-HA-Ub-pLMP2A	Ub-LMP2a-f	CCTGGTCCTGCGTCTGAGAGGTGGTAGCGGATCCTGTCTGGGCGGCCTGCTGACCATGGTGTAAGAATTCACGCGTCTCGAGGCGTGGCC

Table S2. Primers used for qPCR analysis

Gene name	Primer name	Sequence (3’-5’)
MHC-I heavy chain	panHC-RT-f	GGGCTACGTGGACGACAC
	panHC-RT-r	CTCTGGTTGTAGTAGCCGCGC
ORF7a	ORF7a-RT-f	CTTCTGGAACATACGAGGG
	ORF7a-RT-r	CCTCTTGTCTGATGAACAG
GAPDH	GAPDH-RT-f	TCAAGGCTGAGAACGGGAAG
	GAPDH-RT-r	CGCCCCACTTGATTTTGGAG